Naval Research Laboratory
Stennis Space Center, MS 39529-5004

NRL/MR/7175--93-7055

Broad Geoacoustic Assessment of Some Regional Areas

JAMES K. FULFORD

Acoustic Simulation and Tactics Branch
Center for Environmental Acoustics

December 17, 1993

Approved for public release; distribution is unlimited.

REPORT DOCUMENTATION PAGE

Form Approved
OBM No. 0704-0188

1. Agency Use Only *(Leave blank).*	2. Report Date.	3. Report Type and Dates Covered.
	December 17, 1993	Final

4. Title and Subtitle.
Broad Geoacoustic Assessment of Some Regional Areas

5. Funding Numbers.

Program Element No.	0603264N
Project No.	H1292
Task No.	000
Accession No.	DN262105
Work Unit No.	71-5256-03

6. Author(s).
James K. Fulford

7. Performing Organization Name(s) and Address(es).
Naval Research Laboratory
Center for Environmental Acoustics
Stennis Space Center, MS 39529-5004

8. Performing Organization Report Number.
NRL/MR/7175--93-7055

9. Sponsoring/Monitoring Agency Name(s) and Address(es).
Naval Air Systems Command
Code 264G
Washington, DC 20361-1264

10. Sponsoring/Monitoring Agency Report Number.
NRL/MR/7175--93-7055

11. Supplementary Notes.

12a. Distribution/Availability Statement.
Approved for public release; distribution is unlimited.

12b. Distribution Code.

13. Abstract *(Maximum 200 words).*

A broad geoacoustic assessment of three regional shallow-water areas has been made. The geoacoustic properties within each region are mapped into three geoacoustic models representing low (sand-silt-clay), moderate (clayey-silt) and high (silty-clay) bottom loss. Representative extreme sound speed profiles are used to generate a cone of launch angles where the loss is less than a specified amount per bounce. In general, only regions of low loss have good propagation characteristics for each extreme of sound speed.

14. Subject Terms.
Acoustic, ASW, Reverberation, Active, Oceanography, Modeling

15. Number of Pages.
24

16. Price Code.

17. Security Classification	18. Security Classification of Report.	19. Security Classification of This Page.	20. Limitation of Abstract. of Abstract.
Unclassified	Unclassified	Unclassified	SAR

NSN 7540-01-280-5500

Standard Form 298 (Rev. 2-89)
Prescribed by ANSI Std. Z39-18
298-102

DTIC QUALITY INSPECTED 5

BROAD GEOACOUSTIC ASSESSMENT OF SOME REGIONAL AREAS

1.0 INTRODUCTION

This memorandum report documents a broad regional acoustic environmental characterization for the shallow-water areas of the Mediterranean, the Arabian Gulf, the Yellow Sea, Straits of Korea, and Sea of Japan. There are a number of observables that will influence the acoustic characteristics of an area including the sound speed, the bottom characteristics, the wind field, the current field, and the local maritime commerce. Since the focus of this study is on the shallow-water regions, the study will deal only with the sound speed field and the bottom characteristics.

Prior to a characterization of the areas of interest, it is necessary to define the term shallow water. Here, it means the region from the 1500-meter-depth contour to the 30-meter-depth contour. This definition does not restrict shallow water to being strongly bottom interactive. It does restrict shallow water to areas where clastic sediments are being or have been actively deposited.

2.0 METHODOLOGY

The methodology used in the study to characterize a region is based on the regional (or subregional) sound speed field expected extremes and a simple geoacoustic description of the bottom.

The expected sound speed field extremes are the most downward refracting environment, which can occur during the warm season, and the most upwardly (or least downward) refracting environment, which can occur during the cold season. These two extreme environments form the envelope for acoustic performance insofar as sound speed is concerned.

The bottom characteristics will be defined by one of three geoacoustic models. Emery (1969) states that about 70% of the world's continental shelves have been laid down in the past 15000 years. That is, during a

time when the sea level was 100 m lower than it is today. With higher coast lines, the sands of riverine systems were deposited directly on the continental shelves, with the clay and silt materials deposited in the continental-slope environment. Thus, the first model will reflect the coarser materials laid down on the shelves during the last ice age. Green and Matthews (1983) point out that the expected sediment on the continental slope is a clayey-silt, which will be adopted as the model for the continental slope areas. A final model represents the effect of current low energy riverine action (or selective deposition), which is a thin mud veneer overlying the coarser materials. Examples of this environment include the central basin of the Yellow Sea (Nino and Emery 1961), and the regions with less than 40 m water depth off Corpus Christi (Matthews et al. 1985).

3.0 GEOACOUSTIC MODELS

The three geoacoustic models that will be used to characterize the regions are listed in Table 1. The models are a silty-clay representative of Holocene sedimentary covering, a clayey-silt representative of a continental-slope, and a sand-silt-clay model representative of the major sections of the continental shelf. The models are based on a simple shallow-water model suggested by Hamilton (1974) for shallow-water regions. That model consists of a homogeneous layer of material overlying the basement. This model has been adopted with the additional provision that the higher values for attenuation in each material was selected. It is not clear how much energy will be absorbed or scattered, for the purposes of this study; the worst case is assumed for each model. This choice will make each of the models pessimistic rather than optimistic. The bottom loss grazing angle curves for each of the geoacoustic models is generated using REFLEC (Evans 1981), a model based on the Thompson-Haskel matrix formulation for plain wave reflection coefficients for multilayered media.

The silty-clay model is based primarily on two areas, the central basin of the Yellow Sea, and the inner shelf of the Gulf Coast of the United States. Geotechnical data collected by Booth and Winters (1989) in the Yellow Sea Basin adjacent to the Shantung Peninsula suggests that much of the

central basin is covered by a Holocene mud layer less than 3 m thick. The Holocene mud layer off the Gulf Coast is significantly thicker (Matthews et al. 1985); however for 500 to 5000 Hz acoustic energy the acoustic difference will be small. Based on these two points, a surficial mud layer of 5 m was imposed on the model overlying a 195-m-thick layer of sand-silt-clay. There is no basement is this model, instead there is a homogeneous sand-silt-clay half space underlying the sand-silt-clay. Figure 1 shows the bottom loss for the silty-clay model. Note that the bottom loss for the first 15° for 500 and 1000 Hz is similar to a High Frequency Bottom Loss (HFBL) province 2 curve; this result is accidental. Selecting a slightly different Holocene layer thickness will result in other frequencies producing answers near a HFBL province 2 curve.

The clayey-silt model used for the continental slope is an interpretation of the clay-silt composition as documented by Green and Matthews (1983), and generalized velocity ratio charts (U.S. Naval Oceanographic Office, unpublished chart). The basic model is a single layer of clay-silt extending 200 m with a half-space basement of clay-silt. Figure 2 shows the bottom loss for the clay-silt mixture. In the interval from 0 to 10° the loss predicted by this model is less than that predicted by HFBL province 1, and in the interval 0 to 15° the loss is less than that predicted by HFBL province 2.

The sand-silt-clay model is a compromise between a high speed sand and a lower speed sand-silt-clay. The silt reported by Booth and Williams (1989) is representative of high speed material, which agrees with a model verified by comparison with acoustic data from the Korea Straits (Kinney, unpublished manuscript); however, the straits of Hormuz (Gomes et al. 1993) suggest a lower speed for what should be similar material, and White and Klitgord (1976) report the surface sediment compressional velocity to be 1560 m/s off the Makran coast. In compromise, a sound speed ratio (1.04) higher than Hamiltons (1980) sand-silt-clay (1.033) and lower than silt (1.057) has been selected. Figure 3 shows the bottom loss versus grazing angle curves for each of the frequencies, as well as the reference HFBL province 1 and 2 curves. The bottom loss curves for this

material are less than the HFBL curve 1 for the interval of 0 to 14°, and HFBL curve 2 for the interval of 0 to 16° for all frequencies.

Table 1. Geoacoustic models used for broad area environmental characterization (note: each model assumes a water sound speed of 1500 m/s)

	Depth (m)	Acoustic Velocity (m/s)	Attenuation (dB/m-kHz)	Density (g/cm^3)
Silty-Clay model: used to represent a Holocene mud surface layer. Velocity Ratio (sediment to water) equals 0.988.				
	0.0	1491.0	0.06	1.421
	2.5	1493.3	0.06	1.424
	5.0	1497.5	0.06	1.427
	5.0	1555.0	0.15	1.603
	10.0	1561.5	0.15	1.611
	50.0	1605.9	0.15	1.668
	100.0	1666.9	0.13	1.720
	200.0	1789.9	0.11	1.800
Clayey-Silt model: used to represent the continental rise. Velocity Ratio (sediment to water) equals 1.014.	Depth (m)	Acoustic Velocity (m/s)	Attenuation (dB/m-kHz)	Density (g/cm^3)
	0.0	1521.0	0.10	1.488
	2.5	1524.3	0.10	1.491
	5.0	1527.5	0.10	1.494
	10.0	1534.0	0.10	1.502
	50.0	1584.4	0.10	1.560
	100.0	1638.4	0.09	1.595
	200.0	1755.9	0.07	1.713
Sand-Silt-Clay model: used for coarse clastics common to continental shelves. Velocity Ratio (sediment to water) equals 1.040.	Depth (m)	Acoustic Velocity (m/s)	Attenuation (dB/m-kHz)	Density (g/cm^3)
	0.0	1560.0	0.10	1.596
	2.5	1562.3	0.10	1.599
	5.0	1566.5	0.10	1.602
	10.0	1573.0	0.10	1.610
	50.0	1623.0	0.10	1.668
	100.0	1677.4	0.09	1.703
	200.0	1794.9	0.07	1.821

4.0 REGIONAL ANALYSIS

In this section each of the three regions will be analyzed. The analysis will consist of selecting from published sources the extremes of sound speed profiles that are expected for the region. The three geoacoustic models will be mapped onto the bathymetry/physiography of the region. A propagating fan will be predicted for each environment of the region (that is, representative sound speed and geoacoustic area).

This analysis will begin with the Arabian Sea, continue with the Yellow Sea, Straits of Korea, Sea of Japan, and conclude with the Mediterranean Sea.

4.1 Arabian Sea Region

The Arabian Sea region encompasses the area from the Gulf of Aden to Bombay India. The associated continental shelf is variable in width, from a maximum of 300 km offshore of India and West Pakistan to virtually absent off the Makran and Omani coasts. The shelf break typically occurs at a water depth of approximately 200 m.

The major physiographic features of the Arabian Sea region are relics of the rifting of the Indian plate from Madagascar, and the motion of India northward along with the outflow of the Indus River. The rifting episode is delineated in a series of fracture zones and ridge structures that give the major textural features to the continental rises and abyssal plains. The Indus River provided a large part of the terrigenous sediments that accumulated on the continental shelf until its regulation for irrigation and power production purposes. Another primary source of sedimentary material is wind-blown deposits from the Iran-Makran Desert.

Figure 4 shows a map of the Arabian Sea provinced by geoacoustic model applicability. The shelf regions are modeled as a sand-silt-clay mixture. On the basis of similar textural patterns within the region, the compressional velocity of White and Klitgord (1976) has been used as the surface velocity for the entire region. This does not agree with the

analysis of Gomes et al. (1993), which places the shelf regions (with the exception of the Strait of Hormuz and the Indus Fan) as regions of silty-clay. However, based on the U.S. Naval Oceanographic Office sediment velocity ratio map of the area and the White and Klitgord (1976) study, it seems likely that the shelf has a significant sand content. The continental slope region is mapped as a clayey-silt, that is, higher loss than the shelf. No indication of significant deposits of silty-clays in waters deeper than 30 m, or less than 1500 m have been noted; thus, this shallow-water region is mapped without a significant area of high loss. It is probable that high loss areas exist within this region as a result of local depositional or erosional patterns, though these areas should be of limited extent.

Gomes et al. (1993) present a representative selection of sound speed profiles from the Arabian Sea. The sound speed profiles (for water depths less than 1500 m) are usually downward refractive; though, upwardly refractive conditions do exist in the Strait of Hormuz. For the purpose of this study, the sound speeds have been divided into two groups: a group representative of the areas outside of the Strait of Hormuz and a group that represents the Strait of Hormuz. Table 2 lists three representative sound speed profiles for the region outside of the Strait of Hormuz. The three samples represent the two extremes and a median. Table 3 lists two representative sound speed profiles for the Strait of Hormuz.

Table 4 lists the maximum downward (or upward launch) launch angle that intersects the bottom with less than 1 dB and 2 dB per bounce of bottom loss for slope regions. Two water depths are used, 500 m and 1000 m. The table shows that all propagation suffers more than 1 dB per bounce for these environments, and that less than 2 dB per bounce is only possible for frequencies around 100 Hz with a largest maximum launch angle of 15°.

Table 2. Representative sound speed profiles for the Arabia Sea, exclusive of the Strait of Hormuz

Depth (m)	Gulf of Oman (m/s) (N.E. Monsoon)	Makran Coast (m/s) (Spring)	Gulf of Cambay (m/s) (S.W. Monsoon)
0	1533.54	1539.29	1547.12
10	1533.46	1538.47	1545.20
20	1533.33	1537.29	1545.41
30	1533.34	1536.16	1545.55
50	1533.36	1535.18	1544.83
75	1533.51	1534.23	1541.27
100	1530.89	1531.22	1538.63
125	1528.53	1528.41	1534.40
150	1528.16	1525.73	1530.58
200	1530.16	1522.75	1526.32
250	1533.05	1520.43	1522.63
300	1532.32	1518.94	1520.37
400	1514.91	1513.57	1516.25
500	1512.72	1508.55	1512.99
600	1510.41	1506.99	1509.51
700	1508.83	1506.01	1505.54
800	1507.56	1504.94	1503.90
900	1506.44	1503.86	1502.65
1000	1505.30	1502.54	1502.87

Table 5 lists the maximum downward (or upward) launch angle that interacts with the bottom with less than 1 dB per bounce of bottom loss for shelf regions. For the shelf areas outside the Strait of Hormuz, a water depth of 200 m has been assumed, and in the Strait of Hormuz a water depth of 100 m has been assumed. For the purposes of analysis in downward refracting environments, the source/receiver is assumed to be placed at the sound speed maximum. This procedure leads to an underestimate of the width of the energy cone that can be propagated with low bottom loss. In the case of upwardly refracting sound speeds the

source/receiver is placed at midwater column. The table shows that in the worst case scenario, the smallest maximum launch angle is 9°.

Table 3. Representative sound speed profiles for the Strait of Hormuz

Depth (m)	N.E. Monsoon Sound Speed (m/s)	S.W. Monsoon Sound Speed (m/s)
0	1531.06	1549.05
10	1531.27	1548.20
20	1531.54	1548.46
30	1531.75	1548.89
50	1534.18	1540.08
75	1538.75	1536.26
100	1539.14	1535.49

Table 4. Maximum launch angle that interacts with the bottom with less than 1 or 2 dB per bounce for the continental slope areas of the Arabian Sea (0° indicates the absence of angles that interact with less than 1 dB or 2 dB per bounce)

		Gulf of Oman		Makran coast		Gulf of Cambay	
frequency	water depth	1 dB	2 dB	1 dB	2 dB	1 dB	2 dB
100 Hz	500 m	0°	15°	0°	7°	0°	7°
	1000 m	0°	8°	0°	5°	0°	0°
500 Hz	500 m	0°	1°	0°	0°	0°	0°
	1000 m	0°	0°	0°	0°	0°	0°
1000 Hz	500 m	0°	0°	0°	0°	0°	0°
	1000 m	0°	0°	0°	0°	0°	0°
5000 Hz	500 m	0°	0°	0°	0°	0°	0°
	1000 m	0°	0°	0°	0°	0°	0°
HFBL '1'	500 m	0°	0°	0°	0°	0°	0°
	1000 m	0°	0°	0°	0°	0°	0°
HFBL '2'	500 m	0°	0°	0°	0°	0°	0°
	1000 m	0°	0°	0°	0°	0°	0°

The environmental limits of acoustic propagation that can be inferred from this analysis for the Arabian Sea region are as follows: (1)

propagation should not be constrained by bottom loss on the shelf, and (2) propagation in the deeper water will be severely degraded by bottom loss. There are other limits to propagation that have not been quantified, such as coherent loss due to scattering from microtopography of the sedimentary surface, which may be important factors.

Table 5. Maximum launch angle that interacts with the bottom with less than 1 dB per bounce for shelve areas (0° indicates the absence of angles which interact with less than 1 dB per bounce)

	Strait of Hormuz N.E. Monsoon	Strait of Hormuz S.W. Monsoon	Gulf of Oman N.E. Monsoon	Makran coast Spring	Gulf of Cambay S.W. Monsoon
100 Hz	18°	15°	17°	16°	15°
500 Hz	16°	13°	15°	13°	12°
1000 Hz	16°	13°	15°	13°	12°
5000 Hz	15°	12°	13°	11°	11°
HFBL '1'	5°	0°	0°	0°	0°
HFBL '2'	4°	0°	0°	0°	0°

4.2 Korean Seas

The Korean Seas include the Yellow Sea, the Straits of Korea, and the adjacent coastal waters of the Sea of Japan. The Yellow Sea is characterized by a broad flat featureless seafloor, with an average depth of 55 m with maximum depth is less than 100 m (Chough 1983). The western part of the Yellow Sea is bordered by the deltas of the Hwangho and Yangtze Rivers. The eastern part is fringed by numerous islands and tidal flats along the coast. The straits of Korea (also called the South Sea) is deeper (greater than 100 m), and has rock outcrops similar to those occurring in the eastern part of the Yellow Sea. The eastern shelf of the Sea of Japan is rather smooth and deepens toward the continental slope except for a sedimentary feature called the Hupo Bank. The shelf is relatively straight with few embayments.

The distribution of surface sediments on the eastern shelf of Korea are largely sands and muds to water depths of 500 m, after which they

become muds (Chough 1983). The straits of Korea are characterized by poorly sorted muddy sediments (sand gravel silt and mud), except where strong currents have winnowed out the finer materials. The Yellow Sea surface sediments are dominated on the western side by winnowing the fine materials out of the Hwangho and Yangtze sediments; the central area is largely a low density fine grained mud (silty-clay), and the eastern side of the Yellow Sea is dominated by coarser grained material from the Korean uplands. Underlying the surface sediments is a thick layer of tertiary sediments.

Figure 5 shows a map of the Korean Seas provinced into three geoacoustic bottom loss areas. There are two major regions of silty-clay geoacoustic model areas appearing on the map. Both areas are located in the Yellow Sea -- the entire northern region (the Gulf of PoHai) and the central basin of the Yellow Sea. The Gulf of PoHai is a shallow area (less than 40 m) which receives the direct outflow of the Hwangho River. The high loss associated with the central basin is largely a result of the same river. The areas adjacent (toward the Shantung Peninsula and the coast of Korea) have fine grained materials winnowed out by the strong loop extension of the Kurishio Current (Valencia 1987). These adjacent areas, the strait of Korea and the east coast of Korea out to 200-m depth are modeled as being dominated by sand-silt-clay mixture. In the Yellow Sea, measurements by Booth and Winters (1989) show that the actual materials are denser and presumably have higher velocities. The same is true of the Straits of Korea (Kinney, unpublished manuscript), and indications are that the east coast has higher speed sediments (1600 m/s versus 1560 m/s) than this model (Chough 1983). Again the slope, from 200 m to 1500 m is assumed to be clayey-silt.

Table 6 shows regionally representative sound speed profiles for summer and winter. The sound speeds have been divided into two regions. The first region is for the Yellow Sea (including the Straits of Korea), and the second region is for the east coast of Korea.

Table 7 lists the maximum downward (or upward) launch angle that interacts with the bottom with less than 1 dB per bounce of bottom loss

for shelf regions. For the shelf areas on the eastern coast of Korea, a water depth of 200 m has been assumed, and in the Yellow and South Seas a water depth of 100 m has been assumed. For the purposes of analysis in downward refracting environments the source/receiver is assumed to be placed at the sound speed maximum. This procedure leads to an underestimate of the width of the energy cone that can be propagated with low bottom loss. In the case of upwardly refracting sound speeds the source/receiver is placed at midwater column. The table shows that in the worst case scenario, the smallest maximum launch angle is 1° for the sand-silt-clay covered areas and poor propagation for the central basin of the Yellow Sea (the largest silty-clay area). In fact, for the central basin of the Yellow Sea, during the summer each interaction would have a minimum loss of 4 dB per bounce for the geoacoustic model. The summer propagating angles are probably underestimated for the sand-silt-clay areas (low loss), the actual sediment velocity to water velocity ratio is probably 1.06 or greater, suggesting that the propagating angles should be 3 to 5° larger than this table lists.

Table 6. Representative sound speed for the Korea Seas

Depth (m)	Yellow Sea Summer svp (m/s)	Winter svp (m/s)	Sea of Japan Summer svp (m/s)	Winter svp (m/s)
0	1527.05	1471.57	1526.35	1478.81
10	1523.85	1471.97	1521.11	1478.94
20	1517.98	1472.07	1508.53	1479.09
30	1509.18	1472.49	1495.61	1479.20
50	1496.11	1474.00	1478.84	1479.12
75	1484.48	1475.78	1471.37	1477.20
100	1479.34	1476.01	1470.49	1472.26
125	1474.12	1476.23	1468.06	1466.39
150			1464.38	1462.38
200			1455.51	1460.16
250			1455.02	1458.68
300			1455.86	1457.10
400			1457.01	1456.17
500			1458.38	1457.54
600			1459.79	1459.67
700			1461.19	1461.38
800			1462.69	1463.00
900			1464.18	1464.48
1000			1465.77	1465.90

Table 7. Interaction angles with the bottom for the shallow-water regions of the Korean Seas

	Yellow Sea		Sea of Japan		Yellow Sea Central Basin	(silty-clay)
	Summer	Winter	Summer	Winter	Summer	Winter
100 Hz	8°	18°	1°	14°	1°	11°
500 Hz	1°	15°	0°	12°	0°	3°
1000 Hz	1°	15°	0°	11°	0°	3°
5000 Hz	1°	15°	0°	11°	0°	3°
HFBL '1'	0°	4°	0°	0°	0°	3°
HFBL '2'	0°	3°	0°	0°	0°	3°

Table 8 lists the maximum downward (or upward) launch angle that intersects the bottom with less than 1 dB and 2 dB per bounce of bottom loss for slope regions. Two water depths are used, 500 m and 1000 m. The table shows that all propagation above 100 Hz suffers more than 1 dB per bounce for these environments. At 100 Hz a 1° cone exists during winter at 500 m, and a 4° cone exits at 1000 m. At 100 Hz a 11° cone exists at both 500-m and 1000-m depth. Interestingly enough, HFBL province 1 displays the same 2 dB cone for winter sound speed profiles. This is caused by the fact that the clay-silt model and HFBL province 1 both have 2 dB per bounce loss at approximately 14°.

Table 8. Interaction angles with the bottom for continental slope region of the sea of Japan adjacent to Korea

	Summer 500 m		Winter 500 m		Summer 1000 m		Winter 1000 m	
	1 dB	2 dB	1 dB	2 dB	1 dB	2 dB	1 dB	2 dB
100 Hz	0°	0°	1°	11°	0°	0°	4°	11°
500 Hz	0°	0°	0°	0°	0°	0°	0°	0°
1000 Hz	0°	0°	0°	0°	0°	0°	0°	0°
5000 Hz	0°	0°	0°	0°	0°	0°	0°	0°
HFBL '1'	0°	0°	0°	11°	0°	0°	0°	11°
HFBL '2'	0°	0°	0°	0°	0°	0°	0°	0°

The environmental limits of acoustic propagation that can be inferred from this analysis for the Korean Seas are as follows: (1) the central basin of the Yellow Sea and the Gulf of PoHai are extremely bottom limited during normal summer environments, (2) the straits of Korea, and the portions of the Yellow Sea not covered with a thin mud layer are characterized by good propagation for all seasons, (3) the shelf of the eastern coast is more bottom limited than the straits of Korea, and (4) the continental slope regions are intermediate between the clay covered areas and the eastern coast shelf of Korea.

4.3 Mediterranean Sea

The Mediterranean Sea is a region composed of a number of distinct seas (for example, the Cretan, Aegean, Adriatic, Levantine, Alboran, and Balearic), and straits linking these seas. In keeping with the purpose of this report, the key points of the shelves and continental slopes will be reviewed. For a more general overview of the Mediterranean Sea see Null et al. (1992). In general, the continental shelves are wider on the African side. The major depositional feature of the region is the Nile Fan. In most places the sediments of the last 6 million years are underlain by an evaporite sequence, which is the acoustic basement for most areas. The typical shelf sediment is a sand (Keller and Lambert 1972). In the straits regions (Sicily and Gibraltar) it is not uncommon to find ponds of low velocity mud. The continental slopes are typically clayey-silts to sand-silt-mud mixtures (U.S. Naval Oceanographic Office 1970 and DSDP 1970).

Figure 6 shows a map of the Mediterranean provinced into geoacoustic areas. Using a broad brush approach all shelf areas have been mapped as sand-silt-clay mixtures (analysis of sediments off the coast of Libya (U.S. Naval Oceanographic Office 1970), and Sardinia (U.S. Naval Oceanographic Office 1970) show more pure sands). The slopes have been mapped as clayey-silts, which is pessimistic given the analysis of the slopes in the Nile Fan area (DSDP 1970). Areas where silty-clays are known to exist in straits and other protected areas are mapped.

Table 9 lists representative sound speeds for the Mediterranean. Two sound environments have been selected from Null et al. (1992): a Levantine Basin summer profile, which gives the most downward refractive environment, and a winter Strait of Sicily for the most upwardly refractive environment.

Table 9. Representative extreme sound speed profiles for the Mediterranean Sea

Depth (m)	Summer Levantine Basin	Winter Strait of Sicily
0	1540.9	1509.3
10	1540.5	1509.5
20	1537.8	1509.5
30	1531.5	1509.5
50	1524.2	1509.7
75	1520.1	1509.9
100	1519.0	1510.1
125	1518.6	1511.5
150	1518.3	1512.5
200	1517.9	1513.4
250	1517.5	1513.7
300	1517.2	1514.7
400	1517.0	1516.2
500	1517.5	1517.6
600	1518.5	1519.0
700	1519.8	1520.5
800	1521.1	1522.1
900	1522.6	1523.6
1000	1524.2	1525.1

Table 10 lists the interaction angles for the Mediterranean Sea for a summer sound speed environment. In this table, each of the seven environments that exist are listed. The silty-clay environment (or high loss mud bottom) has water depth of 300 m assigned to it; this represents a typical number for the Strait of Sicily. The sand-silt-clay bottom (lowest loss) for the continental shelf is assigned a water depth of 200 m. Interpretation of the interaction angles listed in Table 10 suggests that good propagation will generally be possible in the sand-silt-clay areas during the extreme summer profile.

Table 10. Interaction angles for the summer sound speed profile for the four bottom scenarios in the Mediterranean Sea

	Sand-Silt-Clay	Silty-Clay (300 m)	Clayey-Silt (500 m)		Clayey-Silt (1000 m)	
			1 dB	2 dB	1 dB	2 dB
100 Hz	14°	2°	3°	10°	5°	11°
500 Hz	10°	0°	0°	0°	0°	0°
1000 Hz	9°	0°	0°	0°	0°	0°
5000 Hz	9°	0°	0°	0°	0°	0°
HFBL '1'	0°	0°	0°	10°	0°	11°
HFBL '2'	0°	0°	0°	0°	0°	0°

Table 11 lists the interaction angles for the Mediterranean Sea for a winter sound speed environment. Since the sound speed is upwardly refractive, all of the bottom environmental characterizations predict good propagation.

Table 11. Interaction angles for the winter sound speed profile for the four bottom scenarios in the Mediterranean Sea

	Sand-Silt-Clay	Silty-Clay (300 m)	Clayey-Silt (500 m) 1 dB	Clayey-Silt (1000 m) 1 dB
100 Hz	18°	14°	15°	16°
500 Hz	14°	4°	9°	11°
1000 Hz	14°	4°	8°	10°
5000 Hz	14°	4°	8°	10°
HFBL '1'	4°	4°	6°	8°
HFBL '2'	4°	4°	6°	8°

Analysis of the interaction angles produced for the Mediterranean Sea suggest that: (1) sand-silt-clay areas (the coastal shelves) will have good propagation regardless of season, and (2) the silty-clay (high loss mud regions) and clayey-silts (continental slopes) will have good propagation for higher frequencies (above 100 Hz) only during winter.

5.0 SUMMARY

The regional environmental analysis presented in this study divided the shallow-water regions into three bottom loss types. The types were characteristic of continental shelves, continental slopes, and areas where depositional or erosional patterns have lead to concentration of low speed high loss materials. In general, the areas characterized by coarse clastics (sand-silt-clay) have good propagation (large interaction cones) regardless of season, while the other two types of sedimentary environment are much more sensitive to sound speed changes. That is, continental slope and silty-clay regions will have good propagation only during upwardly refractive sound speed environments.

6.0 ACKNOWLEDGMENTS

This work was sponsored by PMA 264, Mr. Bob Davis, Program Manager, under Program Element 0603254N.

7.0 REFERENCES

Booth, James S. and William J. Winters. 1989. "Geotechnical description of Yellow Sea Sediments with some preliminary geological interpretations," Department of the Interior, U.S. Geological Survey, Woods Hole, MA, Open-File Report 89-149.

Chough, Sung Kwun. 1983. "Marine Geology of the Korean Seas," International Human Resources Development Corporation, Boston, 157 p.

Emery, K.O. 1969. "The Continental Shelves," *Scientific American,* Vol. 221, No. 3, p.106-122.

Evans, R.B. 1981. "REFLEC System Technical Description and Users Guide," Ocean Data Systems Inc. Project No. 1004.

Gomes, Bruce R., Paul J. Bucca, Lt. J. Mark Null, and George P. Cloy, 1993. "Environmental Characterization of the Arabian Sea," Naval Research Laboratory, Stennis Space Center, MS, AEAS Report 92-018.

Green, J.A. and J.E. Matthews. 1983. "Global Analysis of the Shallow Geology of Large-Scale Ocean Slopes," Naval Research Laboratory, Stennis Space Center, MS, NORDA Report 197.

Hamilton, Edwin L. 1974. "Geoacoustic Models of the Sea Floor". in *Physics of Sound in Marine Sediments* ed. Loyd Hampton,(Plenum Press) p. 181-222.

Hamilton, Edwin L. 1980. "Geoacoustic modeling of the sea floor," *Journal of the Acoustical Society of America*, Vol. 68, no. 5, p. 313-1340.

Deep Sea Drilling Project Initial Reports, 1970. Volume XIII, Part I Lisbon, Portugal to Lisbon, Portugal, August-October.

Keller G.H. and D.N. Lambert. 1972. "Geotechnical properties of submarine sediments, Mediterranean Sea," in *A Natural Sedimentation Laboratory,* Stoudsburg (Pennsylvania): Dowden, Hutchinson, and Ross, 765 pp.

Matthews, J.E., P.J. Bucca, and W.H. Geddes. 1985. "Preliminary environmental assessment of the Project Gemini site-Corpus Christi, Texas," Naval Research Laboratory, Stennis Space Center, MS, NORDA Report 120.

Nino, H. and K.O. Emery. 1961. "Sediments of shallow portions of East China and South China Sea," *Geological Society of America Bulletin*, vol. 72 p. 731-762.

Null Mark J., Paul J. Bucca and Bruce R. Gomes. 1992. "Environmental Assessment for Selected Regions in the Mediterranean," Naval Research Laboratory, Stennis Space Center, MS, AEAS Report 92-004.

U.S. Naval Oceanographic Office. 1970. "Mine warfare pilot, Strait of Gibraltar-Rota approaches," Stennis Space Center, MS. SP 923.

U.S. Naval Oceanographic Office. 1980. "Mine warfare pilot, Sardina," Stennis Space Center, MS. SP 923.

Valencia, Mark J.. 1987. International Conference on the Yellow Sea. Occasional Papers of the East-West and Policy Institute. Paper no. 3.

White, R.S. and K. Klitgord. 1976. "Sediment Deformation and Plate Tectonics in the Gulf of Oman," *Earth and Planetary Science Letters*, Vol. 32, p. 199-209.

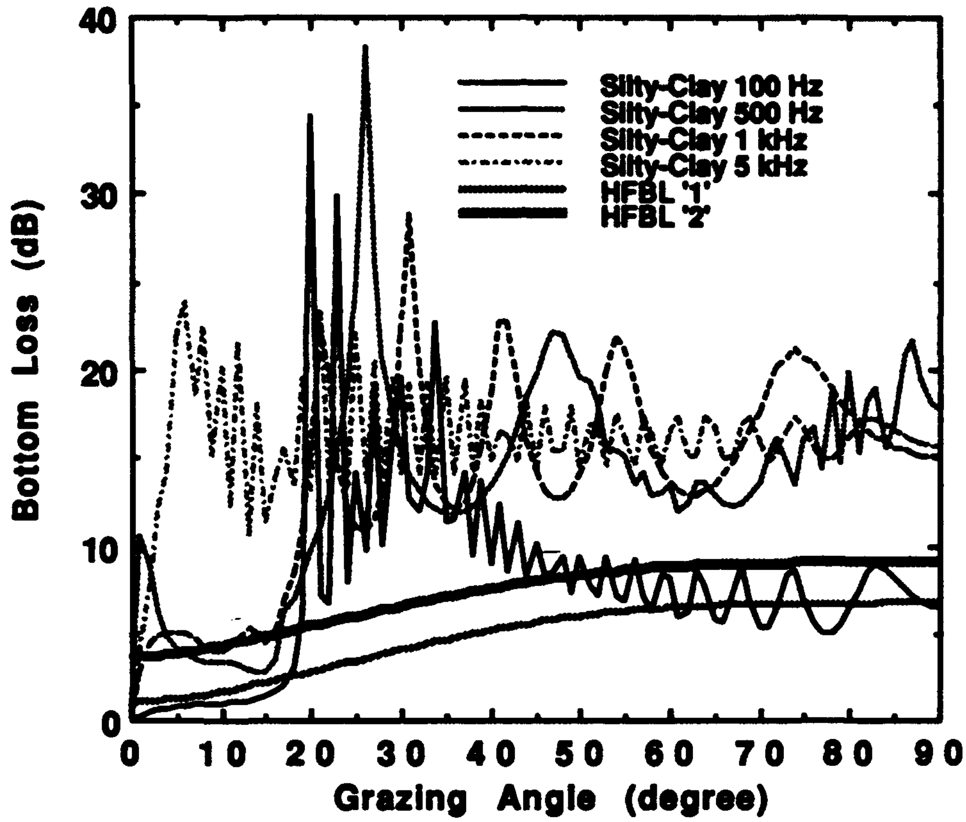

Fig. 1—Plot of bottom loss versus grazing angle for silty-clay geoacoustic model for 100, 500, 1000, and 5000 Hz (HFBL provinces 1 and 2 curves have been added for reference)

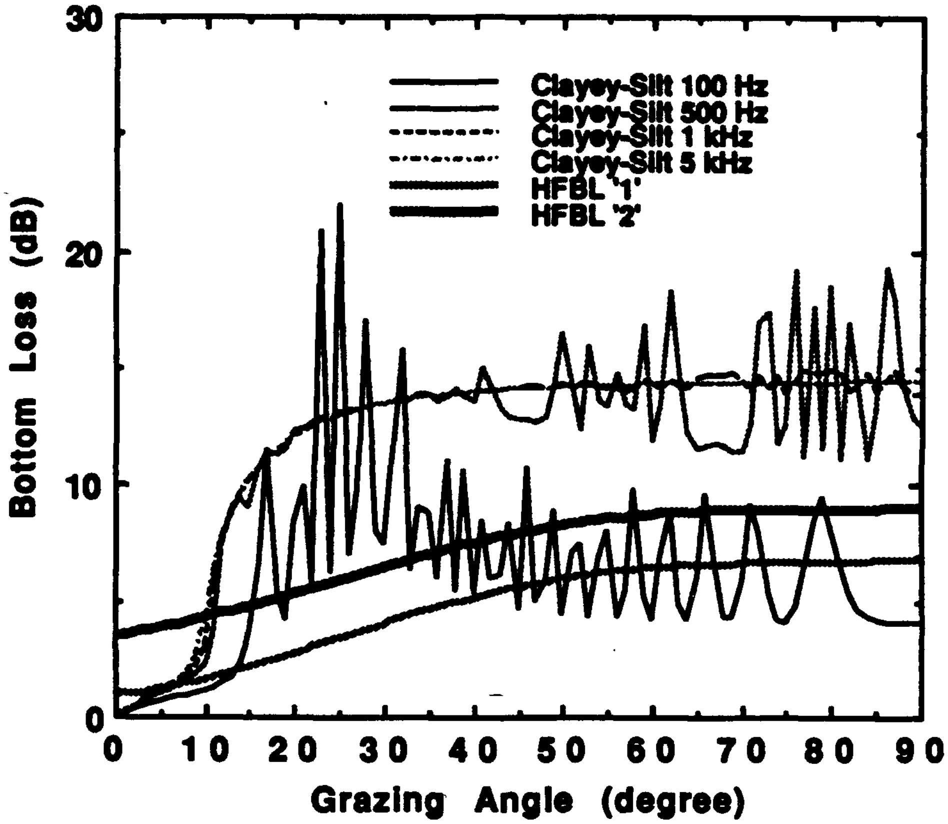

Fig. 2—Plot of bottom loss versus grazing angle for clayey-silt geoacoustic model for 100, 500, 1000, and 5000 Hz (HFBL provinces 1 and 2 curves have been added for reference)

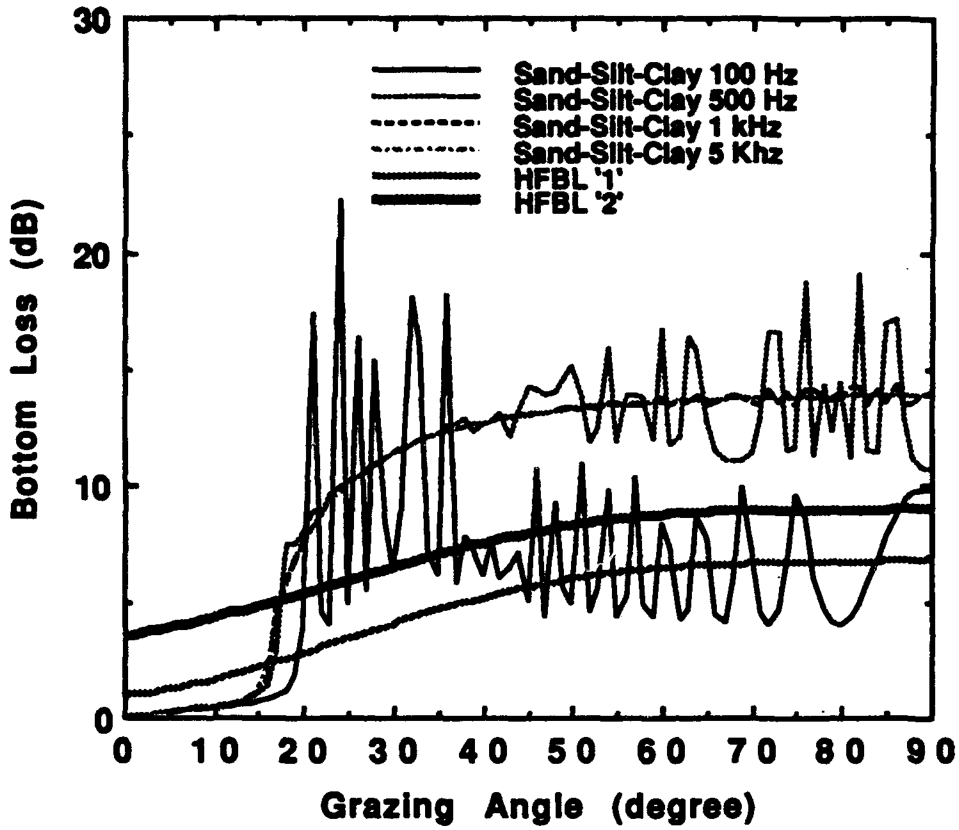

Fig. 3—Plot of bottom loss versus grazing angle for sand-silt-clay geoacoustic model for 100, 500, 1000, and 5000 Hz (HFBL provinces 1 and 2 curves have been added for reference)

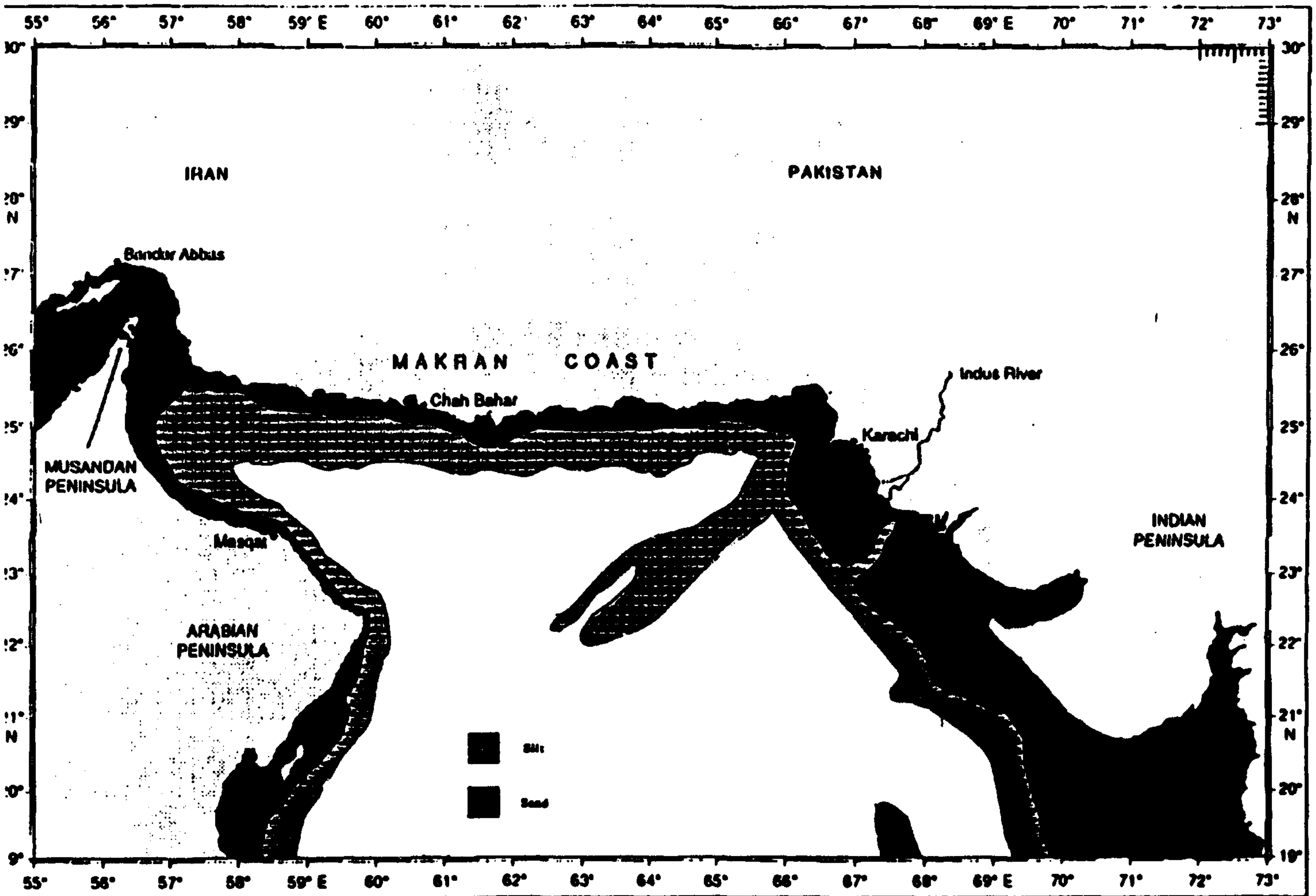

Fig. 4—Plot of Arabian Sea region showing areas of clayey-silt and sand-silt-clay geoacoustic model applicability.

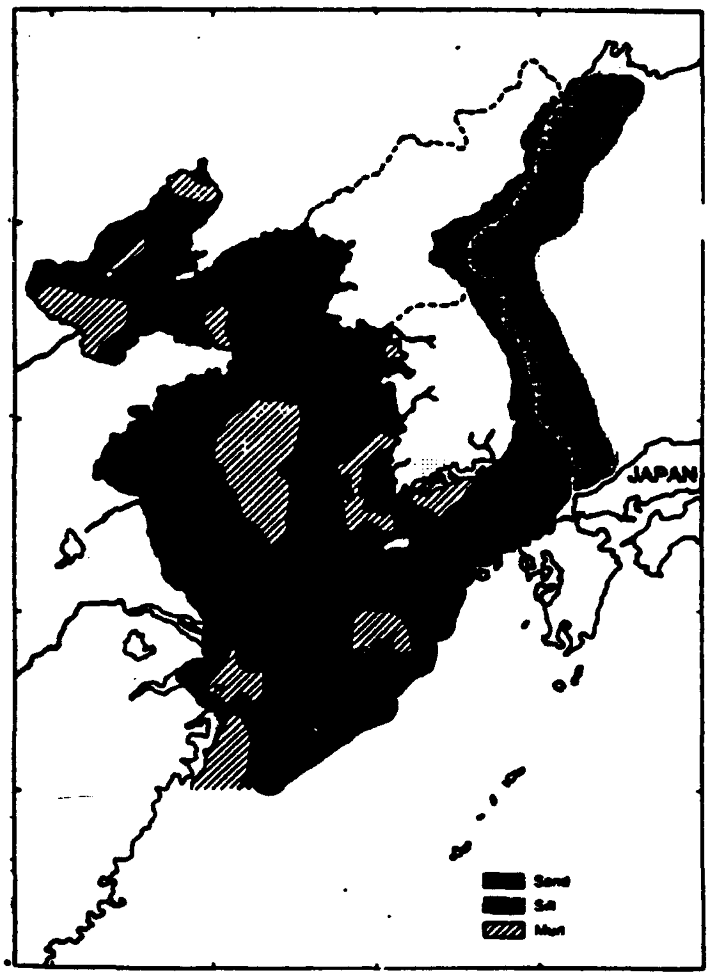

Fig. 5—Plot of Korean Sea region showing areas of clayey-silt, silty-clay, and sand-silt-clay geoacoustic model applicability

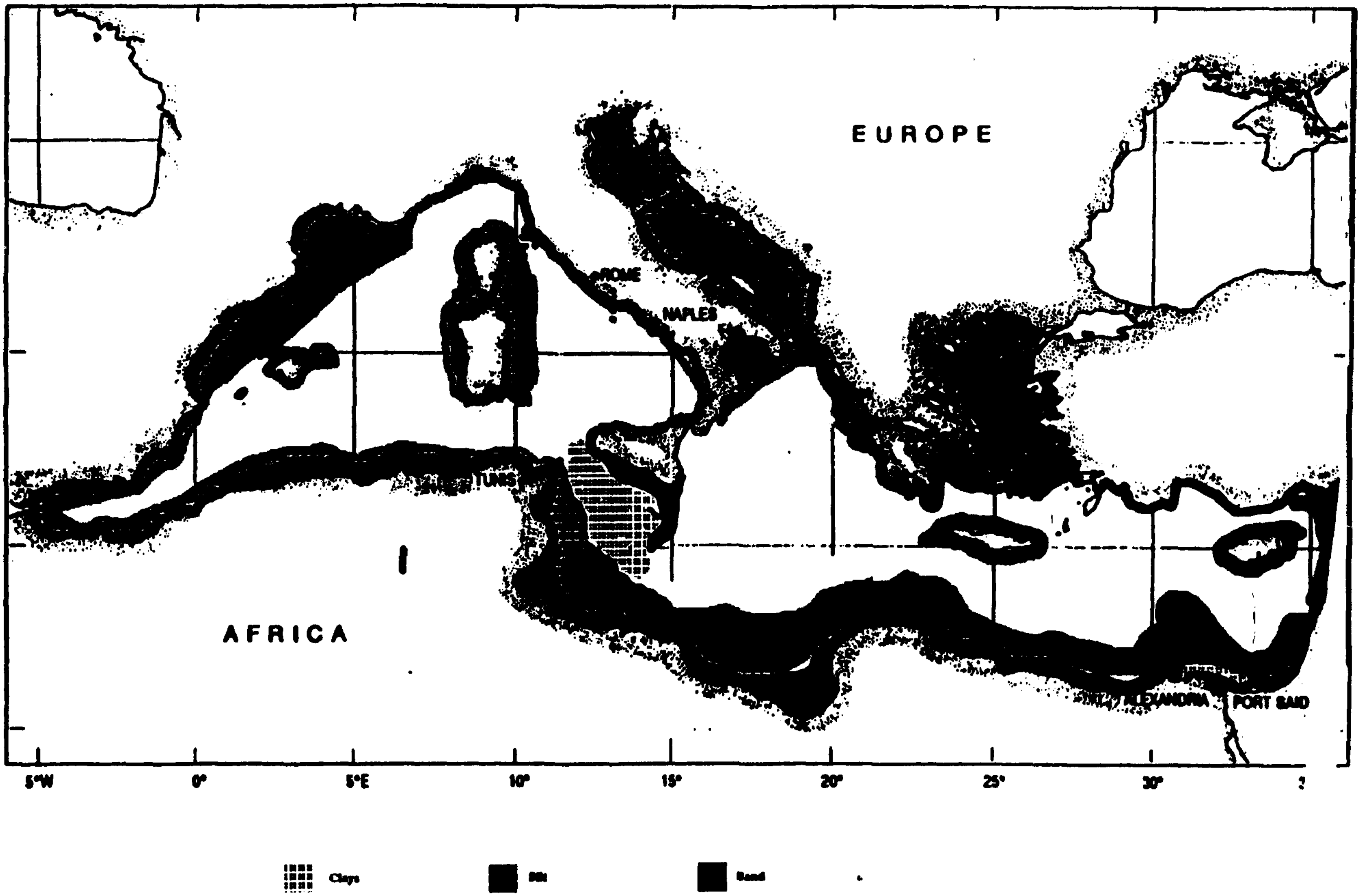

Fig. 6—Plot of Mediterranean Sea region showing areas of clayey-silt, silty-clay, and sand-silt-clay geoacoustic model applicability.